Conformer-Specific Ionization Spectroscopy of Bromocyclohexane: Equatorial versus Axial Conformers

Songhee Han, Hyun Sik Yoo, and Sang Kyu Kim*

Department of Chemistry and KI for Nanocentury, KAIST, Daejeon 305-701, Korea

Received: June 16, 2010; Revised Manuscript Received: August 5, 2010

Ionization of equatorial and axial conformational isomers of the *chair*-bromocyclohexane is investigated with use of the vacuum ultraviolet mass-analyzed threshold ionization (MATI) spectroscopic technique. Two distinct ionization energies of 9.8308 ± 0.0025 and 9.8409 ± 0.0025 eV are determined for equatorial or axial conformers, respectively. From the conformer-selective vibrational analysis, it is found that the equatorial conformer undergoes a drastic structural change upon ionization especially along the C−Br distortion mode, whereas the axial conformer shows the modest change along the ring-puckering mode with ionization, corresponding to the reaction coordinate for the conformational interconversion. Density functional theory (DFT) calculations with and without considering the spin−orbit coupling provide the appropriate mode assignments for the vibrational bands active in the ionization spectra. Natural bond orbital (NBO) analysis is carried out to give insights into the contribution of the anomeric effect to the structure−energy relationship in each conformational isomer.

1. Introduction

Chemical reactivity is strongly dependent on the molecular structure. The reaction outcomes can thus be manipulated if one can select the specific molecular structure of the reactant by any means. This structure-selective reaction control has become reality as some successful experimental studies have been reported recently. These include the conformer-specific photodissociation dynamics of 1-iodopropane ion,[1] propanal ion,[2] and thiophenols.[3] Dissociative ionization of some aliphatic amino acids has also been found to be conformer-specific.[4] In ambient conditions, the molecular structure is often the mixture of many possible structural isomers especially when the barrier for the interconversion of different isomers is low. Conformational isomers belong to this category since the conformational change is induced by the internal rotation about the single bond. Understanding the conformer-specific chemical reactivity is one of the most important keys for unraveling the complex biological problems such as enzyme reactions or protein folding. In the supersonically cooled condition, conformers exist according to their statistical thermodynamic properties, even though it seems to be in controversy whether or not the relative population of the conformers at room temperature remains constant in the supersonic cooling process.[5] In principle, different conformational isomers are separable according to their distinct physical properties, and thereafter, one can further study the chemical reactivity associated with the specific conformational structure.

Cyclohexane and monosubstituted cyclohexanes have long been spotlighted as their equatorial or axial conformational structures provide the prototypical model system for the investigation of the conformer-specific reactivity.[6−16] Bromocyclohexane is a particularly interesting system, as the energy difference between equatorial and axial conformers is small enough for both isomers to coexist in significant amounts at the ambient condition.[17−28] In spite of many studies on the conformational isomerism of bromocyclohexane, its conformer-specific ionization spectroscopy has been little investigated. Recent applications of the vacuum ultraviolet mass-analyzed threshold ionization (VUV-MATI) spectroscopic technique to a number of systems have been very successful in identifying and separating conformational isomers, and these include various conformers of 1-iodopropane, propanal,[29] and alkanethiols.[30] Here, equatorial and axial conformational isomers of the *chair*-bromocyclohexane have been investigated with VUV-MATI spectroscopy to give the accurate ionization energy of each

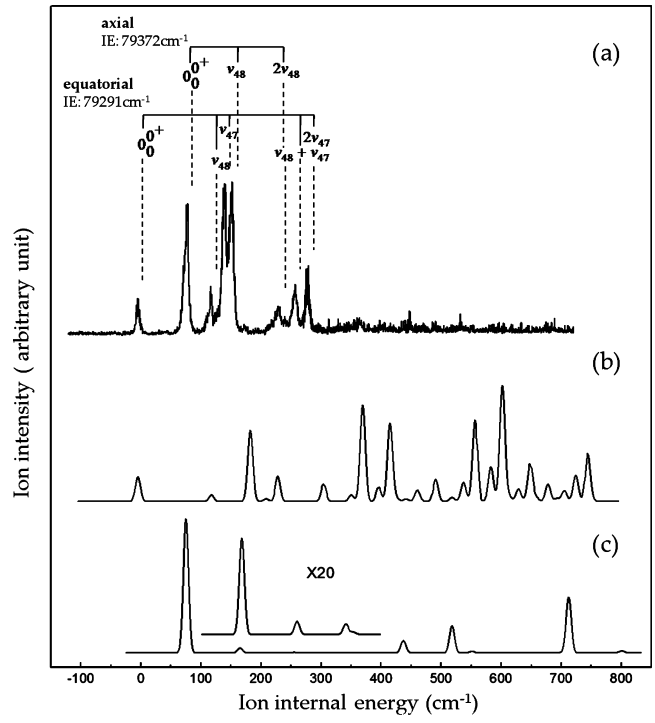

Figure 1. (a) The VUV-MATI spectrum of bromocyclohexane. Franck−Condon simulation spectra based on the B3LYP/6-311++G(3df,3pd) calculations for (b) equatorial and (c) axial conformers.

* To whom correspondence should be addressed. E-mail: sangkyukim@kaist.ac.kr. Fax: (+) 82-42-350-2810. Phone: (+)82-42-350-2843.

10.1021/jp105541v
Published on Web 08/25/2010

TABLE 1: Some of Vibrational Frequencies (cm^{-1}) of Equatorial and Axial Conformers of the *chair*-Bromocyclohexane in the Neutral and Cationic Ground States Calculated at the B3LYP/6-311++G(3df,3pd) Level. The Vibrational Frequencies Obtained by the B3PW91 and PBEPBE Methods with 6-311++G(3df, 3pd) Basis Set are Given in Parentheses (Left: B3PW91, Right: PBEPBE)

	chair-equatorial				*chair*-axial			
	S_0	D_0			S_0	D_0		
	calcd	calcd	expt	description	calcd	calcd	expt	description[a]
ν_{47}	212	187 (179, 149)	145	C−Br distortion	175	163 (162, 154)		C(3,5)H_2 rock
ν_{48}	126	122 (123, 117)	122	ring puckering	114	90 (86, 87)	75	ring puckering

[a] Refer to Table 3 for the atomic labeling.

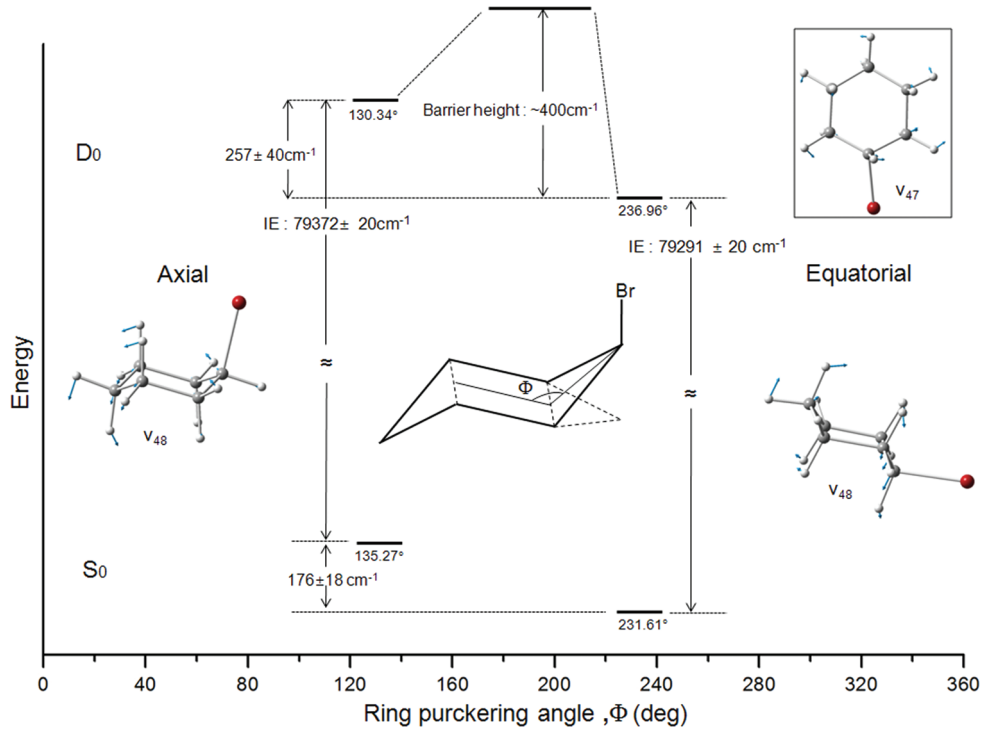

Figure 2. Schematic energetic diagram of axial (left) and equatorial (right) *chair*-bromocyclohexane conformers along the ring puckering conformational angle (Φ). The energy difference between equilibrium structures of two conformers in cationic ground states is determined by using the result of ref 24 for the neutral energy difference and experimental values of IEs from this work. The indicated structural Φ values are determined from the B3LYP/6-311++G(3df,3pd) level calculation. The ν_{47} or ν_{48} normal mode is depicted for each conformer. The barrier height for the conformational interconversion in the cationic ground state is estimated from the MATI spectrum (see the text).

conformer. The experimental result has been analyzed with the aid of theoretical calculations to investigate the origin of the conformational preference, which results from the interplay between anomeric and steric effects.[31]

2. Experimental Section

Bromocyclohexane (Aldrich, 98%) was used without further purification, seeded in the Ar carrier gas, and expanded into the vacuum chamber through a nozzle orifice (General valve, 0.5 mm diameter) with a backing pressure of 1 atm. The resulting supersonic jet was collimated through a 1 mm diameter skimmer (Precision) in a differentially pumped vacuum chamber prior to being overlapped with the counter-propagating VUV laser pulse, which was generated via the four-wave mixing in a Kr gas cell by combining the UV laser pulse fixed at 212.556 nm for the Kr $5p[1/2]_0-4p^6$ transition and the tunable visible (VIS) laser pulse. The dye laser output (Lambda phisik, Scanmate 2) pumped by the third harmonic of a Nd:YAG laser (Continuum, Precision 2) was frequency doubled through a KD*P crystal, rotated by 90° in the linear polarization axis through a $\lambda/2$ waveplate, and frequency-summed with the dye laser fundamental on a BBO crystal to generate the UV laser pulse at 212.556 nm. The VIS laser pulse in the 670−710 nm range for the VUV wavelength tuning was generated by another dye laser (Lumonics, HD-500) pumped by the same Nd:YAG laser. The VUV pulse was spatially separated from UV and VIS fundamentals using the edge of a calcium fluoride (CaF_2) collimating lens placed at the exit of the Kr cell in which the pressure was maintained at ~1 Torr. High-*n*,*l* Rydberg states of molecules generated by the VUV laser pulse were pulsed-field ionized (~10 V/cm) after the delay time of ~20 μs, which is long enough for the complete separation of the MATI ions from the prompt ions along the time-of-flight axis. Therefore, no spoil field was used in this scheme. Generated ions were repelled, accelerated, drifted along the time-of-flight axis, and detected by MCP. Ion signals were digitized by an oscilloscope (LeCroy, LT584M) and stored in a personal computer that was also used for the remote control of all step motors in the experimental setup.

Computational Details. All calculations were carried out with the Gaussian 03W program package.[32] The minimum energy structures and normal modes for ground neutral and

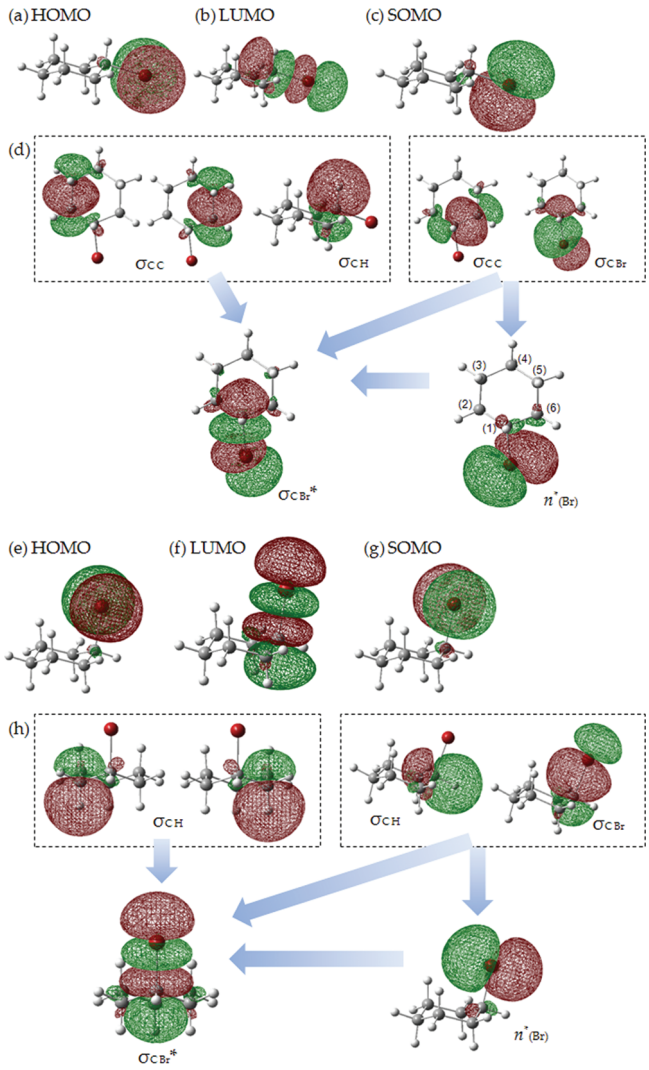

Figure 3. The (a) HOMO, (b) LUMO, and (c) singly occupied molecular orbital (SOMO) of the equatorial conformer are shown with (d) other orbitals showing significant hyperconjugation interactions in the cationic ground state. The (e) HOMO, (f) LUMO, and (g) SOMO of the axial conformer are depicted with (h) hyperconjugating orbitals in the cationic ground state. All orbitals are obtained with NBO calculations at the B3LYP level with the basis set of 6-311++G(3df,3pd). The donor-to-acceptor charge delocalization directions are depicted as arrows.

cationic states were calculated with the B3LYP,[33,34] B3PW91,[35] and PBEPBE[36] density functional theory (DFT)[33,34,36,37] methods with a basis set of 6-311++G(3df,3pd). The Franck−Condon analysis was carried out by using the Duschinsky transformation[38] with a code developed by Peluso and co-workers.[39,40] Natural bonding orbital (NBO) calculations[41] were carried out at the DFT and MP2[42] levels.

3. Results and Discussion

Bromocyclohexane adopts the fully staggered chair form in the ground electronic state. It is well-known that there exist two distinct conformational isomers of the *chair*-bromocyclohexane: in the axial conformer, the Br atom is placed at the axial position whereas it is attached at the equatorial position in the equatorial conformer. Thermodynamic stabilities of these conformers have been investigated in many different environments. In the gas-phase electron diffraction study, using the relative abundance of two conformers, it has been found that the equatorial conformer is more stable than the axial conformer by 176 ± 18 cm^{-1}.[24,28] This energy difference is very low, and thus it is nontrivial to separate out the specific conformer in the ambient condition. In the supersonically cooled condition, however, each conformer is populated with the minimum internal energy, allowing the clear separation of the conformers. The VUV-MATI spectrum of supersonically cooled bromocyclohexane in Figure 1(a) represents ionization dynamics of its equatorial and axial isomers. Apparently, it seems to be not straightforward to assign the observed bands in the VUV-MATI spectrum to each conformer. The intensity of the origin band alone cannot be used as a criterion for the judgment of the conformational assignment, since the sum of all band intensities belonging to each conformer should be compared for the determination of different conformer populations. We have carried out the Franck−Condon analysis based on DFT calculations using the B3LYP method with a 6-311++G(3df,3pd) basis set. The geometries and vibrational frequencies in the neutral (S_0) and cationic (D_0) ground states for each conformer are used for the calculation of Franck−Condon factors in the one-photon ionization. From theory, it is predicted that the equatorial conformer undergoes the large structural change upon ionization, giving the small intensity for the ionization origin of the equatorial conformer. On the other hand, the origin is expected to be strongly observed for the axial conformer from the Franck−Condon calculation. These Franck−Condon analyses strongly indicate that the lowest ionization threshold found at the VUV photon energy of 79 291 cm^{-1} in Figure 1(a) should be ascribed to the $0-0^+$ origin of the equatorial conformer. The intensity of this origin band is relatively weak, and this is consistent with the large structural change of the equatorial conformer upon ionization. The second lowest ionization threshold observed at 79 372 cm^{-1} is most likely due to the $0-0^+$ origin of the axial conformer not only because the energy difference of 81 cm^{-1} is rather low for the vibrational frequency of the equatorial conformer but also because the spectral bands at the high energy region cannot be explainable otherwise. This assignment for two different conformer origins makes perfect sense in the further assignment of other vibrational modes belonging to each conformer.

Accordingly, the ionization energies (IEs) of the equatorial and axial conformers of bromocyclohexane are determined to be 9.8308 ± 0.0025 and 9.8409 ± 0.0025 eV, respectively. Rather large uncertainties of IE values here are ascribed to the broad ionization energy window, due to the strong electric field of 10 V/cm employed in the pulsed field ionization.[43] These values are higher than previously reported theoretical values of 9.75 and 9.78 eV, predicted for respective equatorial and axial conformers.[26] However, the higher IE of the axial conformer than that of the equatorial conformer is consistent with the current experiment. Assignments for vibrationally excited bands are quite straightforward, Figure 1. The peaks located at 145 and 284 cm^{-1} above the origin of 79 291 cm^{-1} are assigned to the fundamental and overtone bands of the C−Br distortion mode (ν_{47}) of the equatorial conformer, respectively. It is quite interesting to note that the B3LYP calculation predicts 187 cm^{-1} for ν_{47} whereas B3PW91 and PBEPBE methods give rise to 179 and 149 cm^{-1}, respectively (Table 1). The PBEPBE calculation is especially in good agreement with the experiment, and this should be the consequence of the inclusion of the exchange-correlation energy in the corresponding functional. This demonstrates that the spin−orbit coupling should be carefully considered for the appropriate prediction of the vibrational frequency especially for the mode involving the heavy

TABLE 2: Total Electronic and Deletion Energies (kcal/mol) for Equatorial and Axial Conformers of *chair*-Bromocyclohexane in the Neutral and Cationic Ground States Obtained from the NBO Calculation at Different Levels of Theory with Electronic Energy Differences (in cm^{-1}) in Parentheses

		S_0		D_0	
		equatorial	axial	equatorial	axial
B3LYP/6-311++G(3df,3pd)	E^a	0	0.99 (344.62)	0	1.90 (665.00)
	E^b	0	1.04 (363.23)	0	1.78 (621.55)
	$E_v^{Del\,c}$	15.16	18.74	31.29	24.45
	$E\sigma'^{\,d}$			7.65	1.46
	En^e			8.75	6.28
MP2/6-311++G(3df,3pd)	E^a	0	0.45 (156.70)	0	0.77 (268.64)

[a] Relative electronic energies with respect to the equatorial conformer in the neutral and cationic ground states with the NBO analysis using the B3LYP method. [b] Relative electronic energies with respect to the equatorial conformer in the neutral and cationic ground states without the NBO analysis, using the B3LYP method. [c] The deletion energy defiend as the difference between the electronic energy before and after the deletion of the σ_{CBr}* orbital. [d] Hyperconjugation energies between the n*(Br) and σ_{CBr}* orbitals. [e] Hyperconjugation energies of equatorial and axial conformers considering the $\sigma_{C(1)C(6)}/\sigma_{C(1)Br}$−n*(Br) or $\sigma_{C(1)H}/\sigma_{C(1)Br}$−n*(Br) interactions, respectively.

TABLE 3: Minimum Energy Structural Parameters (Å, deg) of the Neutral and Cationic Ground States of *chair*-Bromocyclohexane Conformers Calculated at the B3LYP/6-311++G(3df,3pd) Level

	Chair-Equatorial			*Chair*-Axial		
	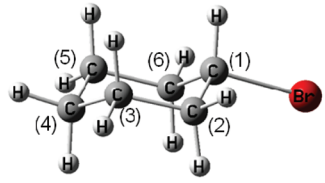			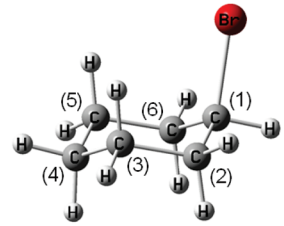		
	S_0	D_0	[a]Diff	S_0	D_0	[a]Diff
R(C(1)-Br)	2.00	1.99	0.47	2.01	1.97	2.10
∠C(2)C(1)Br	110.01	114.37	-3.96	110.12	112.54	-2.20
∠C(6)C(1)Br	110.00	96.92	11.90			
∠HC(1)Br	102.59	104.54	-1.90	101.43	95.55	5.80
∠C(3)C(2)C(1)Br	-179.68	-171.76	4.41	73.37	77.32	-5.38
∠C(5)C(6)C(1)Br	-180.27	-179.30	0.54			

[a] Differences between geometrical parameters of neutral and cation in each conformer according to the equation of (neutral-cation)/neutral × 100.

atom movement.[44] The band at 122 cm^{-1} above the equatorial conformer origin is assigned to the ring-puckering mode (ν_{48}), which matches well with the B3LYP value of 122 cm^{-1}. The 262 cm^{-1} is then ascribed to the $\nu_{48} + \nu_{47}$ combinational mode of the equatorial conformer. For the axial conformer with the origin at 79 372 cm^{-1}, the peak at 75 cm^{-1} above the origin should correspond to the ring-puckering mode (ν_{48}). This agrees well with the B3LYP value of 90 cm^{-1}, indicating that the potential energy surface for the ring-puckering motion is relatively loose for the axial conformer compared to that in the equatorial conformer. The broad band centered at 152 cm^{-1} above the axial origin should then be due to the overtone of ν_{48}.

Although overall spectral features of the MATI spectrum in the low internal energy region are quite well explainable by the Franck−Condon analysis based on DFT calculations as above, some experimental findings are very different from theory, Figure 1. For instance, the Franck−Condon simulation predicts a number of strong vibrational bands in the high internal energy region whereas there is a sudden truncation of the signal at ∼400 cm^{-1} above the ionization origin of the equatorial conformer. This could be due to the complete neglect of the conformational interconversion process in our Franck−Condon simulation. Namely, since the barrier for interconversion between equatorial and axial conformers in the cationic *chair*-bromocyclohexane is low, the vibrational excitation above the barrier may induce the conformational isomerization, which could be responsible for the sudden truncation of the MATI signal. Provided that this scenario works, the barrier height for the conformational change from the equatorial to axial is estimated to be ∼400 cm^{-1} whereas that from the axial to equatorial conformers would be ∼150 cm^{-1} in the cationic state (Figure 2).

The experimental finding that the IE of the equatorial conformer is 81 cm^{-1} lower than that of the axial conformer indicates that the relative stabilization energy of the equatorial conformer with respect to the axial conformer is larger in the cationic state compared to that in the neutral ground state. This observation is in good agreement with the theoretical values predicted by B3LYP or MP2 methods. The extent of the charge delocalization is closely related to the stabilization energy induced by the so-called anomeric effect. This anomeric effect, from our NBO analysis, is found to be mainly induced by the charge delocalization into the C−Br antibonding orbital (σ_{CBr}*), of which the spatial distribution is almost the same as that of the lowest unoccupied molecular orbital (LUMO), Figure 3. For the quantitative analysis, we calculated the deletion energies (E_v^{Del}), which represent the electronic total energies excluding

the σ_{CBr}* orbital, for equatorial and axial conformers in neutral and cationic ground states. The B3LYP value of E_v^{Del} with a 6-311++G(3df,3pd) basis set is smaller by 3.58 kcal/mol for the equatorial conformer compared to that of the axial conformer in the neutral ground state, whereas the deletion energy of the equatorial conformer in the cationic ground state is calculated to be quite larger than that of the axial conformer by 6.84 kcal/mol (Table 2). This big difference of the deletion energy strongly indicates that the anomeric effect through the charge delocalization into the σ_{CBr}* orbital is mainly responsible for the larger stabilization energy of the equatorial with respect to the axial conformer in the cationic state, compared to that in the neutral ground state, giving the smaller IE for the equatorial conformer.

The ionization-driven structural change is also conformer-specific. As indicated in the MATI spectrum, the C−Br distortion mode (ν_{47}) is strongly activated for the equatorial conformer whereas the ring-puckering mode (ν_{48}) is enhanced as the axial conformer is ionized. This conformer-specificity is relevant to the hyperconjugation energy ($E\sigma'$), of which the main contribution is the anomeric interaction between n*(Br) and σ_{CBr}* orbitals, Figure 3. The $E\sigma'$ value for the equatorial conformer in the ground cationic state is calculated to be 7.65 kcal/mol, whereas the axial conformer cation is stabilized by the hyperconjugation energy of 1.46 kcal/mol in terms of the orbital overlap of n*(Br) and σ_{CBr}*, Table 2. It is interesting to note that the n*(Br) orbital of the equatorial conformer is asymmetrically oriented with respect to the C−Br bond axis, and this is probably responsible for the strong activation of the C−Br distortion mode in the corresponding MATI spectrum.

It is noteworthy that the C(1)−Br bond lengths are slightly decreased upon ionization for both equatorial and axial conformers, Table 3. As depicted in Figure 3, the highest occupied molecular orbital (HOMO) has a nodal plane along the C(1)−Br bond and the deficiency of the electron in HOMO should result in the decrease of the antibonding character, thus shortening the C(1)−Br bond upon ionization for both conformers. The HC(1)Br bent angle, ∠HC(1)Br, is increased upon ionization for the equatorial conformer whereas it is decreased as the axial conformer is ionized. The hyperconjugation energy between σ bonding and n*(Br), En, seems to be most responsible for this particular conformer-specific structural change. Namely, according to our NBO analysis, the hyperconjugation energy due to the interaction of $\sigma_{C(1)C(6)}/\sigma_{C(1)Br}$ and n*(Br) is calculated to be 8.75 kcal/mol for the equatorial conformer. On the other hand, the hyperconjugation energy of the $\sigma_{C(1)H}/\sigma_{C(1)Br}$ and n*(Br) interaction is calculated to be 6.28 kcal/mol for the axial conformer. This conformer-dependent hyperconjugation energy difference suggests that the charge density localized in the C(1)−Br bond might increase relatively more in the equatorial conformer compared to that in the axial conformer. In this respect, the ∠HC(1)Br increases upon ionization for the equatorial conformer due to the increased steric effect, whereas it is the opposite case for the axial conformer ionization. From our NBO analysis, it is found that the n*(Br) orbital plays an important role in the structural change upon ionization with the conformer-specificity in terms of the structure-sensitive anomeric interaction.

4. Summary

In this work, using the VUV-MATI spectroscopic technique, the ionization energies of equatorial and axial conformers of the *chair*-bromocyclohexane are accurately determined to be 9.8308 ± 0.0025 and 9.8409 ± 0.0025 eV, respectively. From the vibrationally resolved MATI spectrum in which each band is classified into a specific conformer, it has been found that the equatorial conformer undergoes a drastic structural change upon ionization whereas only a modest structural distortion is observed for the axial conformer. The detail NBO analysis provides the quantitative explanation for the experiment in terms of the anomeric and steric effects. Conformer-specific spectroscopic and dynamic features provide quite valuable information for the understanding of the structure−reactivity relationship, and need to be intensively investigated.

Acknowledgment. This work was supported by the National Research Foundation (2010-0015031, 2010-0000068, 2010-0001635, 2009-0082847).

References and Notes

(1) Park, S. T.; Kim, S. K.; Kim, M. S. *Nature* **2002**, *415*, 306.
(2) Kim, M. H.; Shen, L.; Tao, H.; Martinez, T. J.; Suits, A. G. *Science* **2007**, *315*, 1561.
(3) Lim, J. S.; Lee, Y. S.; Kim, S. K. *Angew. Chem., Int. Ed.* **2008**, *47*, 1853.
(4) Choi, K.-W.; Ahn, D.-S.; Lee, J.-H.; Kim, S. K. *Chem. Commun.* **2007**, *9*, 1041.
(5) Florio, G. M.; Christie, R. A.; Jordan, K. D.; Zwier, T. S. *J. Am. Chem. Soc.* **2002**, *124*, 10236.
(6) Zheng, C.; Subramaniam, S.; Kalasinsky, V. F.; Durig, J. R. *J. Mol. Struct.* **2006**, *785*, 143.
(7) Wilson, M. A.; Chandler, D. *Chem. Phys.* **1990**, *149*, 11.
(8) Strauss, H. L.; Pickett, H. M. *J. Am. Chem. Soc.* **1970**, *92*, 7281.
(9) Sirjean, B.; Glaude, P. A.; Ruiz-Lopez, M. F.; Fournet, R. *J. Phys. Chem. A* **2006**, *110*, 12693.
(10) Pierce, L.; Nelson, R. *J. Am. Chem. Soc.* **1966**, *88*, 216.
(11) Pierce, L.; Beecher, J. F. *J. Am. Chem. Soc.* **1966**, *88*, 5406.
(12) Kuharski, R. A.; Chandler, D.; Montgomery, J. A.; Rabii, F.; Singer, S. J. *J. Phys. Chem.* **1988**, *92*, 3261.
(13) Kakhiani, K.; Lourderaj, U.; Hu, W. F.; Birney, D.; Hase, W. L. *J. Phys. Chem. A* **2009**, *113*, 4570.
(14) Jensen, F. R.; Bushweller, C. H.; Beck, B. H. *J. Am. Chem. Soc.* **1969**, *91*, 344.
(15) Fernández-Alonso, M. d. C.; Cañada, J.; Jiménez-Barbero, J.; Cuevas, G. *Chem. Phys. Chem.* **2005**, *6*, 671.
(16) Damiani, D.; Ferretti, L. *Chem. Phys. Lett.* **1973**, *21*, 592.
(17) Reeves, L. W.; Stromme, K. O. *Can. J. Phys.* **1960**, *38*, 1241.
(18) Eliel, E. L.; Martin, R. J. L. *J. Am. Chem. Soc.* **1968**, *90*, 682.
(19) Reisse, J.; Stien, M. L.; Gilles, J. M.; Oth, J. F. M. *Tetrahedron. Lett.* **1969**, 1917.
(20) Holly, S.; Jalsovszky, G.; Egyed, O. *J. Mol. Struct.* **1982**, *79*, 465.
(21) Woldbaek, T. *Acta. Chem. Scand. A* **1982**, *36*, 641.
(22) Damiani, D.; Scappini, F.; Caminati, W.; Corbelli, G. *J. Mol. Spectrosc.* **1983**, *100*, 36.
(23) Caminati, W.; Damiani, D.; Scappini, F. *J. Mol. Spectrosc.* **1984**, *104*, 183.
(24) Shen, Q.; Peloquin, J. M. *Acta Chem. Scand., Ser. A* **1988**, *42*, 367.
(25) Kolodziejski, M.; Waliszewska, G.; Abramczyk, H. *Chem. Phys.* **1996**, *213*, 341.
(26) Tian, S. X.; Kishimoto, N.; Ohno, K. *J. Electron Spectrosc. Relat. Phenom.* **2002**, *125*, 205.
(27) Carrera, A.; Mobbili, M.; Moriena, G.; Marceca, E. *Chem. Phys. Lett.* **2008**, *467*, 14.
(28) Durig, J. R.; El Defrawy, A. M.; Ward, R. M.; Guirgis, G. A.; Gounev, T. K. *J. Mol. Struct.* **2009**, *918*, 26.
(29) Choi, S.; Kang, T. Y.; Choi, K.-W.; Han, S.; Ahn, D.-S.; Baek, S. J.; Kim, S. K. *J. Phys. Chem. A* **2008**, *112*, 5060.
(30) Choi, S.; Kang, T. Y.; Choi, K.-W.; Han, S.; Ahn, D.-S.; Baek, S. J.; Kim, S. K. *J. Phys. Chem. A* **2008**, *112*, 7191.
(31) *The Anomeric Effect and Associated Stereoelectronic Effects*; Thatcher, G. R. J., Ed.; American Chemical Society: Washington, DC, 1993.
(32) Frisch, M. J.; Trucks, G. W.; Schlegel, H. B.; Scuseria, G. E.; Robb, M. A.; Cheeseman, J. R.; Montgomery, J. A., Jr.; Vreven, T.; Kudin, K. N.; Burant, J. C.; Millam, J. M.; Iyengar, S. S.; Tomasi, J.; Barone, V.; Mennucci, B.; Cossi, M.; Scalmani, G.; Rega, N.; Petersson, G. A.; Nakatsuji, H.; Hada, M.; Ehara, M.; Toyota, K.; Fukuda, R.; Hasegawa, J.; Ishida, M.; Nakajima, T.; Honda, Y.; Kitao, O.; Nakai, H.; Klene, M.; Li, X.; Knox, J. E.; Hratchian, H. P.; Cross, J. B.; Bakken, V.; Adamo, C.; Jaramillo, J.; Gomperts, R.; Stratmann, R. E.; Yazyev, O.; Austin, A. J.; Cammi, R.; Pomelli, C.; Ochterski, J. W.; Ayala, P. Y.; Morokuma, K.; Voth, G. A.; Salvador, P.; Dannenberg, J. J.; Zakrzewski, V. G.; Dapprich, S.; Daniels, A. D.; Strain, M. C.; Farkas, O.; Malick, D. K.; Rabuck, A. D.; Raghavachari, K.; Foresman, J. B.; Ortiz, J. V.; Cui, Q.; Baboul, A. G.;

Clifford, S.; Cioslowski, J.; Stefanov, B. B.; Liu, G.; Liashenko, A.; Piskorz, P.; Komaromi, I.; Martin, R. L.; Fox, D. J.; Keith, T.; Al-Laham, M. A.; Peng, C. Y.; Nanayakkara, A.; Challacombe, M.; Gill, P. M. W.; Johnson, B.; Chen, W.; Wong, M. W.; Gonzalez, C.; Pople, J. A. *Gaussian 03W*; Gaussian, Inc., Wallingford, CT, 2004.

(33) Lee, C.; Yang, W.; Parr, R. G. *Phys. Rev. B* **1988**, *37*, 785.

(34) Becke, A. D. *J. Chem. Phys.* **1993**, *98*, 5648.

(35) Perdew, J. P.; Wang, Y. *Phys. Rev. B* **1992**, *45*, 13244.

(36) Perdew, J. P.; Burke, K.; Ernzerhof, M. *Phys. Rev. Lett.* **1996**, *77*, 3865.

(37) Becke, A. D. *Phys. Rev. A* **1988**, *38*, 3098.

(38) Duschinsky, F. *Acta Physicochim. URSS* **1937**, *7*, 551.

(39) Peluso, A.; Santoro, F.; Re, G. D. *Int. J. Quantum Chem.* **1997**, *63*, 233.

(40) Borrelli, R.; Peluso, A. *J. Chem. Phys.* **2003**, *119*, 8437.

(41) Glendening, E. D. R., A. E.; Carpenter, J. E.; Weinhold, F. *QCPE Bull.* **1990**, *10*, 58.

(42) Möller, C.; Plesset, M. S. *Phys. Rev.* **1934**, *46*, 618.

(43) Merkt, F. *Annu. Rev. Phys. Chem.* **1997**, *48*, 675.

(44) Lee, M.; Kim, H.; Lee, Y. S.; Kim, M. S. *Angew. Chem., Int. Ed.* **2005**, *44*, 2929.

JP105541V